Sticking and scattering in the molecular chemisorption regime: CO on Pt(111)

J. Harris
Institut für Festkörperforschung der KFA, D-5170 Jülich, Federal Republic of Germany
A. C. Luntz
IBM Almaden Research Laboratory, San Jose, California 95120

(Received 17 July 1989; accepted 1 August 1989)

The nondissociative sticking of CO on Pt(111) has been measured as a function of incident energy and angle. Both these sticking measurements and prior molecular beam scattering experiments are incompatible with simple theoretical models that describe successfully weak physisorption interactions. For strong chemical interactions, such as for CO–Pt(111), lateral and rotational corrugations in the interaction potential are large and play an important role in the scattering and sticking. Both translational to rotational and normal to parallel energy conversions cause substantial energy scrambling in the interaction. Classical trajectory calculations that incorporate these effects realistically predict a rather gentle fall off in sticking with incident energy, a scaling of sticking with total rather than normal energy and directly scattered distributions which consist of broad lobular components about the specular superimposed on an even broader diffuse component. All of these findings are in accord with experiment.

I. INTRODUCTION

When a weakly interacting atom collides at low incident energies with a solid surface, i.e., when the interaction is dominated by physisorption forces, the incident particle exchanges energy with the surface mainly by excitation or deexcitation of surface and bulk phonons. In such cases, simple classical one dimensional models have been reasonably successful in describing the general features of the dynamics.[1] In the so-called soft-cube model, for instance, the atom with incident energy E_i and incident angle θ_i collides with a smooth part of the surface which is connected to the bulk via a spring. Only the normal component of incident energy $E_n = E_i \cos^2 \theta_i$ is available to excite the lattice. The magnitude of the energy transfer between particle and surface (Δ) determines the outcome of the collision. If Δ exceeds E_n, the particle will be trapped in the atom–surface potential well and stick to the surface. On the other hand, if $\Delta < E_n$, the atom will reflect from the surface with an energy loss from E_n of Δ. Since the parallel component of energy is conserved the emergent angle is supraspecular and determined solely by Δ (at zero surface termperature). Recent measurements of the angular distributions of scattered rare gas atoms, although showing some deviations from the predictions of the soft-cube model, nevertheless support the assumption of the dominance of E_n in determining Δ.[2,3]

Because of this apparent dominance of E_n in the direct inelastic scattering, it has long been assumed that the sticking is also dependent primarily on the normal energy, i.e. that the sticking coefficient S scales with E_n. While this seems consistent with the known weak lateral corrugations of physisorption potentials, a number of recent experiments[4–6] have shown that S scales neither with E_n nor with the total energy E_i, but is a nonseparable function of both incident energy and angle. Theoretically, this has been discussed in detail in terms of the distinction between trapping ($E_n < 0$) and sticking ($E_i < 0$).[6,7] Particles which initially trap can either lose parallel momentum via inelastic processes and eventually stick or scatter back into the gas phase by converting parallel to normal momentum via elastic processes. On weakly corrugated surfaces, scattering into either channel is fairly weak. However, both channels are roughly equivalent, and it is the relative and not the absolute strengths of the two channels that determines the overall dependence of S on the incident conditions. When the incident particle is a molecule rather than an atom, excitation of internal degrees of freedom can be important, even for weakly interacting systems. In particular, the conversion of translational to rotational energy has been well studied in scattering experiments by using laser probes to measure the internal state distribution of scattered molecules.[8] While there are still some questions of detail with respect to conversion processes, the sticking and scattering behavior of systems displaying interactions of the physisorption type, whether in the classical or quantum regimes, is in reasonable accord with the predictions of simple models or perturbation theory.

When strong chemical interactions between an incident molecule and surface are involved ($\simeq 1$ eV), the scattering and sticking problem is considerably more complex. Nonadiabatic behavior is more likely and electron–hole pairs could play a significant role in dissipating initial energy. Sticking often involves dissociation of the molecule. In these cases sticking experiments can be instrumental in understanding bond-breaking processes at surfaces. When dissociation does not occur, the interaction will nevertheless depend in a non-trivial way on the orientation of the molecular bond and the impact parameter with respect to the surface mesh,i.e., the adiabatic potential energy surface (PES) is expected to display relatively strong rotational and lateral

corrugations. In addition, the large well depth implies a strong coupling to the lattice which will, in general, be influenced by the rotational corrugation. In such circumstances, simple models are unlikely to give an accurate picture of the scattering process and its outcome.

In this paper, we consider the molecular chemisorption regime explicitly taking the system CO on Pt(111) as an example. We report sticking measurements for CO on Pt(111) that span the range of incident energies 0.05–3.5 eV and incident angles 0°–60°. These measurements show two qualitative differences from previous measurements on physisorption systems. First, the sticking persists to considerably higher incident energies, far beyond the estimates of soft-cube models. Second, S is practically independent of incident angle, i.e., S scales rather well with the total energy of the incoming molecule, E_i. These features will be shown to result from the strong rotational and lateral corrugations of the molecule–surface interaction and are expected to be quite general for molecular chemisorption systems.

The CO–Pt(111) system was chosen for this study primarily because of the wealth of data that is already available. Previous molecular beam studies, for example, have demonstrated that the sticking coefficient of CO on the uncovered surface at $E_i \simeq 0.05$ eV is $\simeq 0.85$ at $T_s = 300$ K,[9] and that S is only weakly dependent on T_s.[9–11] For the particles that do not stick, the scattering distribution at large θ_i is characterized by a dominant lobular pattern ($\simeq 40°$ FWHM) superimposed on a weak broad background.[9,11]. This background was cited as evidence for desorption from a physisorbed state,[11] which is hard to reconcile with the lack of evidence for a precursor mechanism for sticking on the bare surface. As we show below, the observed angular patterns can be accounted for without involing a separate physisorption state and in a manner which is in accord with a direct sticking into the chemisorption well. By contrast, the Kisliuk-like coverage dependence of S and the dominance of a trapping–desorption component in scattering from the CO covered surface, do point to a precursor mechanism for CO sticking on CO covered Pt(111).[9,11]

The organization of the rest of this paper is as follows. In Sec. II A we describe the experimental arrangements and procedure used to measure the sticking coefficient. The results of the measurements are then presented in Sec. II B and compared with other data taken for systems displaying a similar type of interaction. The implications of the data and the picture of the scattering process they imply are then discussed in detail with the aid of trajectory calculations in Sec. III. The main conclusions of our work are then given in summary form in Sec. IV.

II. STICKING MEASUREMENTS

A. Experimental

The experimental apparatus and many of the experimental techniques used to measure sticking have been described previously[4,12] and will not be repeated here. The Pt(111) crystal used in these studies was oriented to within 0.5° of the (111) face as determined by Laue back reflection of x-rays. The crystal was cleaned by standard procedures of repeated oxidation–anneal and sputter–anneal cycles until all surface impurities were less than 1% as determined by Auger spectroscopy.

The measurements of nondissociative sticking were performed using the method of King and Wells.[13] Briefly, a triply differentially pumped supersonic nozzle beam of CO initially strikes a quartz plate in front of the Pt(111) surface and the partial pressure of CO in the UHV chamber is measured with a RGA. Since CO does not stick on the quartz, this establishes a pressure P_0 corresponding to zero sticking. Rapid removal of the quartz plate allows the beam to strike the surface and results in a transient decrease in the partial pressure of CO $\Delta P(t)$ due to sticking on the surface. The ratio $\Delta P(0)/P_0$ is an absolute measure of the sticking coefficient at zero coverage S_0. Since the vacuum time constant of the chamber is $\simeq 0.7$ s, the measurement of $\Delta P(0)$ is averaged over several seconds. Since the sticking coefficient of CO on Pt(111) is quite high, the flux of the CO beam is strongly reduced in order to insure that S_0 is in fact measured. This is accomplished both by using seeded beams of $\simeq 1\%$ of CO in various gasses and by reducing the duty cycle of the beam to 2.5% with a chopper.

Beam energies were varied by a combination of heating the supersonic nozzle and by seeding dilute fractions of CO in Ar, He, or H_2. The beam energies were measured to $\simeq 2\%$ accuracy using time of flight techniques with a flight path of 120 cm. Typical energy dispersions (FWHM) were 10%–20% depending upon the exact nozzle conditions.

In an attempt to measure dissociative chemisorption of CO on Pt(111), the C coverage on the Pt(111) was measured for various exposures of a high energy CO beam. The C coverage at the center of the beam was estimated from the ratio of the C(272 eV)/ Pt(237 ev) Auger peak heights.[12] For these experiments, $T_s = 500$ K. This T_s is considerably above the desorption temperature for molecular CO, but below that where the recombination reaction $O(a) + C(a) \rightarrow CO(g)$ occurs.[14,15] Thus, the net result of dissociative chemisorption would be to form adsorbed C and O at this T_s. With metallic nozzles, some CH_4 is produced as a contaminant in the molecular beam via the catalytic reaction $CO + H_2$ when the nozzle temperature is greater than 700 K. Since CH_4 dissociatively chemisorbs on Pt(111) at high kinetic energies to form adsorbed C, such contamination must be avoided in the studies of CO dissociative chemisorption. In order to form high energy beams of CO seeded in H_2 without CH_4 contamination, an alumina nozzle was constructed by laser drilling a $\simeq 100$ μm diameter hole in a thinned portion of the end of a $\simeq 0.65$ cm diameter closed alumina tube. The end of the tube, in the region around the hole, was heated by radiation from a surrounding Ta tube which in turn was heated by RF induction from a water cooled coaxial coil. The approximate temperature of the nozzle was monitored with a $W/5\%$Re–W/26%/Re thermocouple mounted on the Ta tube near the nozzle hole. Temperatures of > 1400 K are readily obtained with a RF power input of $\simeq 400$W. At such nozzle temperatures, no CH_4 contaminant is formed in the alumina nozzles. Because of slip, the CO translational energy was limited to $\simeq 3.5$ eV as determined by the TOF measurements.

B. Results

The dependence of S_0 at $T_s = 350$ K on E_i at $\theta_i = 0°$ and 60° is given in Fig. 1. Results for angles between 0° and 60° were intermediate between these two curves.

In the limit $E_i = 0, S_0 = 0.88$ and is independent of θ_i. The value we observe at $E_i = 0.06$ eV is in excellent agreement with the value obtained previously by Campbell, *et al.*[9] at $T_s = 300$ K. Since S_0 decreases $\simeq 15\%$ with T_s between 90 to 300 K,[10] we anticipate that the low E_i limit of S_0 at $T_s \simeq 0$ K is 1.0. This is entirely reasonable for sticking directly into a deep chemisorption well since steric and impact parameter constraints on the sticking are negligible for $E_i = 0$. The decrease of the sticking with T_s at low E_i is a well known consequence of energy transfer from the surface to the incident particle, and is evident even in simple cube models of the sticking.[16]

The gradual decrease in S_0 with E_i that is evident in Fig. 1 is, however, inconsistent with the simple one dimensional cube models. These predict a step decrease at $E_i \simeq 0.7$ eV for $T_s = 0$ K which becomes somewhat rounded for finite T_s. This gradual decrease in S_0 with E_i is similar to previous observations of CO sticking on Ni(100).[17] It is, however, qualitatively different from the behaviour reported previously for CO sticking on Ni(111).[18] We cannot rationalize the latter observations in terms of the physics described in the next section.

It is also evident in Fig. 1 that the sticking is nearly independent of θ_i, i.e., that the sticking scales approximately with E_i. This is consistent with previous observations for the sticking of N_2 on W(100)[19] and for CO sticking on Ni(100).[17] In the latter case, S_0 actually decreases with θ_i for large E_i.

We also wish to stress that no dissociative chemisorption was observed for any E_i produced ($\leqslant 3.5$ eV). Based on the Auger S/N limits, we estimate that the CO dissociation probability is $< 10^{-3}$ even at $E_i = 3.5$ eV. Since the endothermicity of the dissociation on Pt(111) is at most 1.5 eV, this result demonstrates that translational activation is not effective in promoting dissociation. A similar conclusion was reached for CO dissociation on Ni(111).[20] In addition, no dissociation was observed on Pt(111) at defects at any E_i. Again, this is similar to observations for Ni(111),[20] although Steinrück, *et al.*[21] did observe an energy independent CO dissociation on Ni(100) defects. In contrast to the low reactivity of these metals, it has been proposed that translationally activated dissociation readily occurs for CO on Cu(110),[22] although this has not yet been confirmed in other experiments.

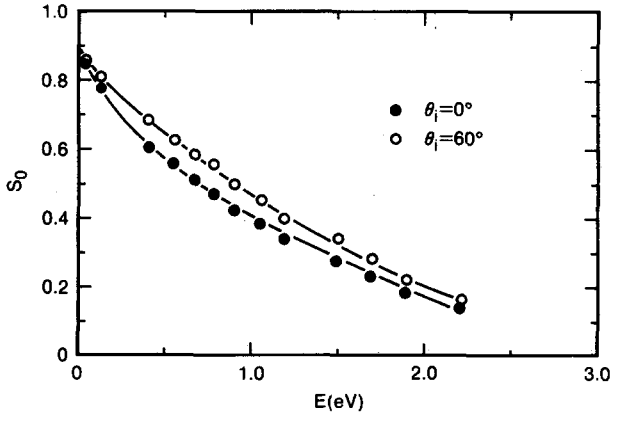

FIG. 1. The sticking coefficient at zero coverage S_0 for CO incident on Pt(111) at $T_s = 350$ K vs incident energy E. The solid points are for $\theta_i = 0°$ and the open circles are for $\theta_i = 60°$. The curves through the points have no theoretical significance.

III. DISCUSSION

In this section we use a simplified classical-trajectory model to interpret and discuss the sticking and scattering results for CO on Pt(111). In view of the large binding energy (1.4 eV) and the participation of the $^2\pi^*$ resonance of CO in the bonding, some electronic nonadiabaticity is certainly anticipated. We will find, however, that the main features of the experiments can be interpreted satisfactorily in terms of adiabatic collisions governed by a single PES having reasonable properties. Thus, there is no compelling reason to believe that electronic nonadiabaticity is a dominant factor in the interaction.

A. General remarks: Inadequacy of soft-cube models

As mentioned in Sec. I, trapping and scattering of incident particles on a lattice is usually discussed in terms of the magnitude of energy transfer (Δ) occurring during the first round trip within the molecule-surface well. If Δ exceeds the normal component of incident energy E_n, the particle will trap on the backswing and may ultimately stick to the surface. If Δ is $< E_n$, the particle will scatter inelastically from the surface. For a collision at normal incidence Δ is found to depend approximately linearly on the energy $\Delta = a + bE_n$, where a and b are constants that depend on the masses, the molecule–surface well depth and the vibrational frequencies of the lattice. Assuming a perfectly flat surface, the sticking coefficient is unity for E_n below the critical energy $E_c = a/(1-b)$, and is zero above this energy. For parameters appropriate to CO/Pt(111), E_c is around 0.7 eV. The data in Fig. 1, showing a smooth falloff of the sticking coefficient over $\simeq 1$ eV, are obviously at variance with this idealized flat-surface model. In addition, the scattered angular distributions[9,11] do not display simple supraspecular lobes and are therefore also at variance with one-dimensional models of the scattering. These models fail because the lateral and rotational corrugations of the PES are strong and give rise to a very substantial conversion of the initial normal kinetic energy into parallel kinetic and rotational energy. A crude argument as to the effect of conversion mechanisms suggests that they should enhance the sticking on the grounds that the conversion increases the time the particle spends in intimate contact with the lattice, and this should result in a net increase in the average energy transfer. This argument is somewhat simplistic and can be, in some circumstances, even completely fallacious because the couplings are strong and cannot be regarded as acting independently. To illustrate the combined effects of strong

corrugations and coupling to the lattice, we consider a classical model that, although oversimplified with respect to the actual scattering system of interest, nevertheless contains the important factors in an integral and realistic fashion.

B. Model PES for CO–Pt(111)

Our model PES for the CO–Pt scattering system is two-dimensional and represents the "substrate" by an array of nine Pt atoms (Fig. 2) which interact mutually via harmonic forces. The force constant is chosen so that the bandwidth of an infinite linear chain is approximately equal to the bandwidth of the bulk phonon bands of Pt[23] [$k = (1/4)M_{Pt}\omega^2$, with $\omega = 25$ meV]. This array does not represent correctly any particular "cut" through the Pt(111) surface but is chosen so that each of the three surface atoms in the "strike zone" has three nearest neighbors connected by springs. The CO is treated as a rigid rotor that interacts with each of the five surface Pt atoms via a two-body potential of the form

$$V = F(V_r F - 2V_0), \tag{1}$$

with $V_r = V_0[1 + \mu(1 - \cos\gamma)]$ and $F = \exp[-\beta(R_i - R_0)]$. γ is the CO bond orientation with respect to the line joining the centers of mass, of length R_i. The parameters V_r and V_0 govern the strengths of the repulsive and attractive parts of the interaction, respectively. The repulsive branch depends on the CO bond angle via the orientational parameter γ such that the CO axis tends to orient along the radius vector with the C atom closest to the Pt. The orientation with the O atom closest to the Pt is the least stable configuration. This rotational corrugation decreases with R_i simulating the weak dependence of the long-range attractive tail on the bond-orientation. If $\mu = 0$, V is simply a Morse potential with depth V_0 and equilibrium distance R_0. The range of the potential is determined by the exponent β, and the value $\beta = 1$ a. u. was used in all calculations.

When single-site potentials of the form Eq. (1) are summed in the geometry of Fig. 2, the orientational dependence of the potential depends on lateral position in a nontrivial way. If the CO center of mass lies over the central atom of the cluster, the interaction with this atom dominates and the bond axis tends to align along the normal with the C atom down. If the lateral position is slightly displaced, the central atom interaction remains dominant and the CO tends to line up along the radius vector joining the centers of mass of the CO and the central atom, i.e., to become slightly tilted with respect to the surface normal. Towards a bridge site, two nearest-neighbor interactions are equally important and the CO cannot orient optimally with respect to both sites. The bond axis then tilts back and points along the normal, optimizing the mismatch with respect to each of the sites. This behavior is similar to that found in electronic structure calculations of the interaction of CO with aluminium cluster.[24] A further feature of the model interaction is that the repulsive wall is softer for the bridge site than for the on-top site. This is in agreement with the lower Pt–CO stretch frequency in the bridge site relative to the on-top site. The strength of the lateral corrugation of the potential is governed by the parameter R_0. This corrugation decreases with the normal distance from the surface as expected. Thus, although highly simplified, V does contain many essential features of the correct PES.

Calculations were performed using the two sets of potential parameters tabulated in Table I. Also included in this table are the well depths and corrugations that result when the lattice sum is carried out over the cluster. Except for the choice of V_0, which was adjusted to give a reasonable chemisorption well depth ($\simeq 1.3$ eV) no attempt has been made to tailor the PES by fitting to observed site-dependent energies or vibrational frequencies. In particular, the lateral variation of V is not correct in detail, since various studies show that the on-top and bridge site adsorption energies are nearly equivalent. Details on an energy scale of order 0.1 eV are, however, quite unimportant with regard to the scattering and sticking of particles with energies in the eV range. Potential II corresponds to a PES qualitatively similar to that used in previous studies[25,26] and thought to represent a reasonable approximation to the true CO/Pt(111) interaction. Potential I, included solely for comparison purposes, is rotationally uncorrugated and has about the same lateral corrugation as II.

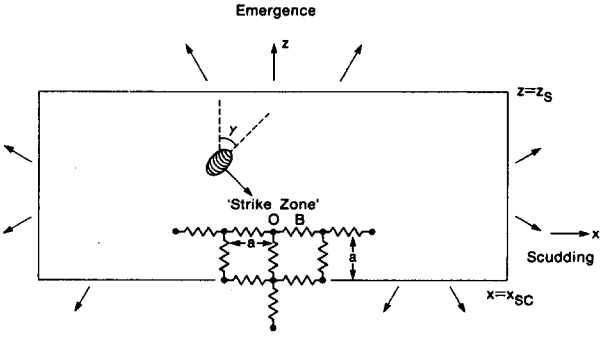

FIG. 2. Schematic diagram of the theoretical model used to calculate sticking and scattering of CO from a Pt surface. The ellipse represents the CO at orientation to the surface normal. The solid points represent the Pt substrate atoms coupled by harmonic forces. The points O and B are used to approximate on top and bridge sites, respectively, for the true Pt(111) surface. The lines about the cluster illustrate the planes used to define the emergent and scudding fractions.

C. Details of the trajectory calculation

Classical trajectories using these two potentials were started at a surface–molecule distance $Z_s = 14$ a.u., where the interaction is essentially zero. Averaging over initial orientation was with respect to cos γ, i.e., a phase space appropriate for a three dimensional rotor. Impact parameters were chosen to mimic averaging over the primitive two dimensional unit cell, i.e. between bridge sites about the central atom (the strike zone). As truncation conditions we required,

(i) recrossing of the line $Z = Z_s$ (emergence),

(ii) $2N$ changes of sign in the normal component of the centre of mass velocity (sticking),

(iii) crossing one of the lines $X = \pm X_{sc}$ or $Z = -a$ (scudding). Here X_{sc} is a distance much larger than the lattice spacing, and we have set this equal to 32 a.u. Scudding trajectories were those that left the cluster either around it's

TABLE I. Parameters of potentials I and II. $V(\gamma)$ gives the well depth for CO bond-orientation γ. The normal distance of the potential minima from the surface are quoted in parenthesis (a.u.). The corrugation height, h, refers to the normal distance between the locations of the 3 eV contour at the on top and bridge sites (O and B in Fig. 2).

				On top			Bridge			
	V_0 (eV)	R_0 (a.u.)	μ	$V(0)$	$V(\pi/2)$	$V(\pi)$	$V(0)$	$V(\pi/2)$	$V(\pi)$	h(a.u.)
(I)	0.8	6.0	0.0	−1.25	−1.25 (5.9)	−1.25	−1.69	−1.69 (5.4)	−1.69	0.5
(II)	0.9	4.7	1.25	−1.24 (4.6)	−0.60 (5.4)	−0.40 (5.8)	−1.56 (4.2)	−0.84 (4.8)	−0.56 (5.3)	0.6

sides, or at very flat emergent angles. In general it is not possible to decide whether, on an infinite array, these trajectories scatter or stick. Accordingly, we count them separately and define three coefficients, P_e, P_s, or P_{sc} according to the number of times each truncation condition was invoked. P_s and $P_s + P_{sc}$ are then taken as lower and upper bounds for the sticking coefficient on an infinite lattice. These limits are, of course, not rigorous but serve to define a region where the sticking coefficient is expected to fall.

D. Sticking probability

Figure 3 shows the expected behavior of the sticking coefficient S for potential I, where the rotational coupling is zero, as a function of E_i and for angles of incidence $\theta_i = 0°$ 3(a) and $\theta_i = 45°$ 3(b). If we consider only trajectories where the CO strikes the central Pt atom head on, the sticking coefficient would be a theta function with edge at 0.7eV [dot–dashed line in Fig. 3(a). Averaging over impact parameter gives the upper and lower bounds for S referred to above, $P_s + P_{sc}$ and P_s, respectively. The cross-hatched area is for $N = 2$, and the shaded area is the extension of the lower bound that results when N is increased to 4. The increase in N did not influence the upper limit because no trajectories that made two round trips emerged on subsequent round trips. In fact, except for a small band of energies around 1.4 eV, no trajectory that trapped on the first round trip was found to emerge subsequently. The dip in S around 1.4 eV is due to some re-emergence of trapped particles at these energies and is a feature of the lateral corrugation and the precise manner in which the particles bounced from the back wall of the potential. As expected, increasing the number of allowed round trips from 2 to 4 increases the scudding vs the sticking. At low E_i, this is quite dramatic. However, it is very likely that most of the particles that make two round trips before scudding would actually stick on an infinite substrate since they have made three impacts with the surface. Accordingly, we expect the true S to fall within the cross-hatched area corresponding to $N = 2$. The averaging over the impact parameter leads to a rounding of the theta function for S at low E_i and a trailing towards higher E_i. The rounding occurs because particles that hit near a bridge site couple less effectively to phonons than particles that hit on top. The tailing is due to normal-parallel translational energy conversion on the first round trip, which reduces emergence following initial impact viz a viz a perfectly flat surface. For the most part, scudding trajectories corresponded to extremely efficient normal–parallel energy transfer with the particle reflecting from the 'wall' of the surface potential on initial collision at angles close to 90°.

Figure 3(b) shows the equivalent S vs E_i for $\theta_i = 45°$ with $N = 2$. Except for the enhanced scudding, especially at

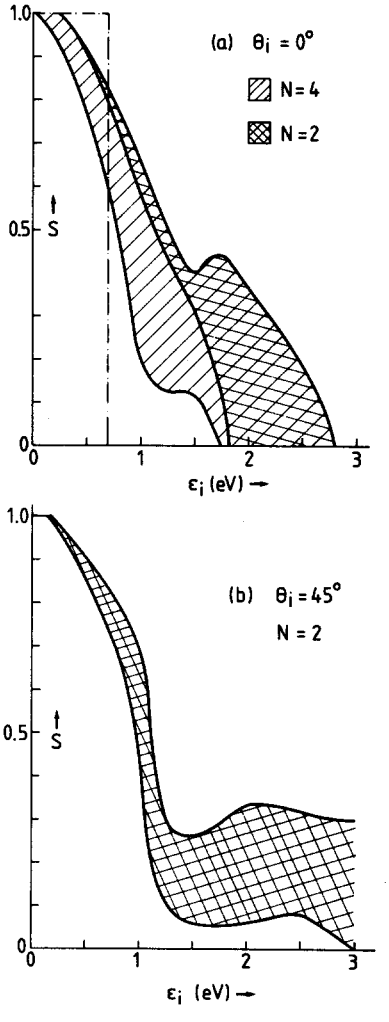

FIG. 3. Sticking calculated for CO–Pt interaction potential I. S is the sticking coefficient and ϵ_i is the initial energy. (a) is for $\theta_i = 0°$ and (b) is for $\theta_i = 45°$. The cross hatched region assumes $N = 2$ as a criteria for sticking while the diagonally shaded area is the extension to the lower bound for $N = 4$.

large incident energies, there is no marked difference in the way S falls off with E_i for the two incident angles. Thus, the Pt array does not display flat surface behavior, i.e., a scaling of S with the normal rather than the total energy. This is because, (a) on the scale of energies of order 1 eV the surface is not particularly flat and (b) the refractive effect of the deep well substantially lessens the influence of incident angle on the actual impact conditions.

Figure 4 shows the sticking behavior calculated for potential II and illustrates the effect of the rotational corrugation on the sticking. In contrast to the results for potential I, many trajectories were found to emerge after making two or more round trips in the well. Many particles trap on the first round trip via translational–rotational conversion but then undergo a reverse transfer and escape. Accordingly, $N = 4$ was used as the criterion for sticking. We noted above that translational–rotational conversion might be expected to enhance S by allowing the molecule to spend more time interacting with the lattice. Comparing Fig. 4 with Fig. 3, we see that S is enhanced only at large energies. For energies up to about 1 eV, S is actually smaller in the presence of translational–rotational coupling than in its absence. This complex behavior results from the fact that translational–rotational conversion causes two competing effects. One is that such conversion increases the number of round trips within the well and thus can enhance energy loss to phonons (the time delay argument). The second is that such conversion reduces energy transfer to phonons in the first round trip since rotational motion is only weakly coupled to the phonon system. The net consequence to sticking depends on which of the two is most important. At low incident energy, the second effect dominates since (in the absence of rotational conversion) most particles lose enough energy on the first round trip to stick. At high incident energy, the first effect dominates since (in the absence of rotational conversion) most particles have enough energy after the first round trip to emerge. We note that the reduction in the first round trip inelasticity via rotational excitation is consistent with the anticorrelation between rotational energy and the energy lost to phonons observed in scattering experiments for NO–Ag(111).[27]

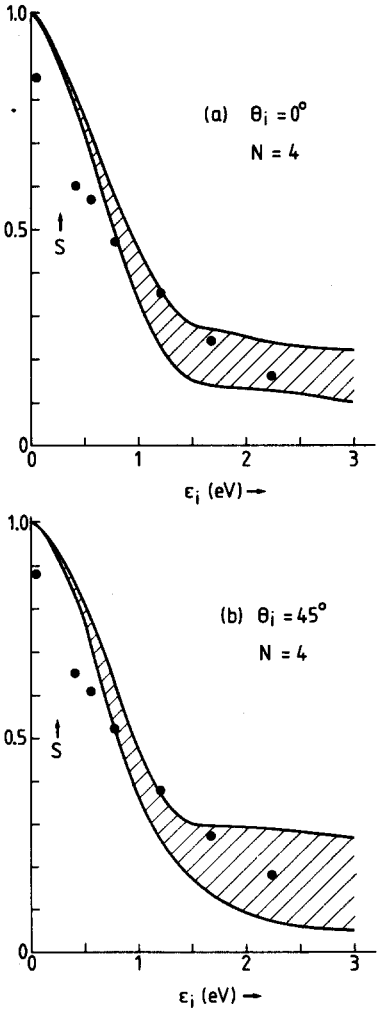

FIG. 4. Sticking calculated for CO–Pt interaction potential II. S is the sticking coefficient and ϵ_i is the initial energy. (a) is for $\theta_i = 0°$ and (b) is for $\theta_i = 45°$. The cross hatched region assumes $N = 4$ as a criteria for sticking. The solid points are experimental results for S_0 at $T_s = 350$ K.

Figure 4(b) gives the expected behavior of S for potential II at an incident angle $\theta_i = 45°$. There is increased scudding as compared with normal incidence, but it is clear that S shows no marked dependence on incident angle throughout the entire energy range considered. Thus, the rotational and lateral corrugations of potential II, which we believe are quite realistic, suffice to scramble the incident energy efficiently and give a sticking behavior that displays something close to total energy scaling. The points in Fig. 4 are experimentally determined values of S_0. These agree reasonably with the bounds of S calculated for potential II. Thus, the results obtained with this potential are consistent with the experimental data, both with respect to energy and angle dependence. The discrepancy at very low incident energy is presumably due to surface temperature effects which are neglected in the calculation.

E. Scattering distributions

Figure 5 shows angular distributions for backscattered particles, as given by potential II with $E_i = 1$ eV at normal incidence [Fig. 5(a)] and for $\theta_i = 60°$ [Fig. 5(b)]. The distributions give the number of trajectories emerging in bins at equal intervals of 5° and refer to probability, not current density. Only particles that emerged [criterion (i) above] were included. The absence of scudding trajectories means that the number of trajectories emerging at very wide angles is underestimated in the figure. The upper curve is normalized to unity and refers to trajectories that emerged up to and including the fourth round trip. The lower curve refers to trajectories that emerged after only one round trip. The numbers emerging after round trip 1–4 were, respectively, 862, 710, 166, 78 at normal incidence and 727, 849, 142, 44 at wide-angle incidence (out of a total 3200 trajectories run in each case). For wide incident angle, the distribution [Fig. 5(b)] displays a broad maximum in the neighborhood of the specular direction. This is sometimes taken to imply a flat surface in the sense that a relatively large number of trajec-

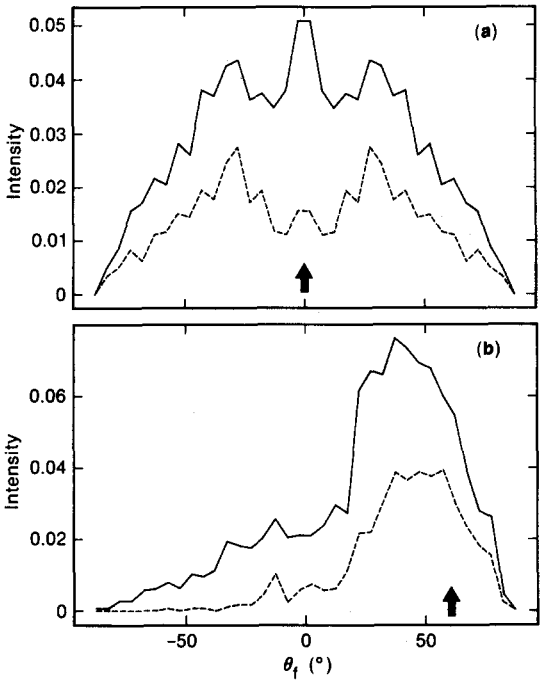

FIG. 5. The scattered angular distribution calculated for potential II for (a) $\theta_i = 0°$ and (b) $\theta_i = 60°$. The intensity is the fraction of total trajectories having the emergence truncation condition in a 5° wide bin and θ_f is the final scattered angle. In (a) and (b) the dashed curve is for particles emerging after one round trip in the well, while the solid curve is for all particles emerging with $N \leqslant 4$. The arrow marks the specular direction.

tories undergo specular reflection. As the distribution for normal incidence shows, however, [Fig. 5(a)] the surface is in no sense flat and the occurrence of a near-specular lobe at wide-angle incidence is merely a sign that the incident parallel energy is less efficiently converted or dissipated than the normal energy. A part of the parallel energy is retained throughout the collision and gives a bias, or skew to the resulting angular distributions of emerging molecules.

In addition to the main lobe, the wide incidence total scattering distribution exhibits a broad background. This is a common feature of measured angular distributions and is usually interpreted in terms of trapping desorption. That is, the lobe in the forward direction is attributed to particles which scatter directly from the surface and the background to particles that trap for relatively long times and are then re-emitted as a result of a thermal fluctuation. The calculations presented above show that for the chemical interaction considered, matters are considerably more complex and direct scattering contributes not only the lobe, but a substantial background as well. The background arises primarily from trajectories that make more than one round trip in the well. Each traverse of the well causes a scrambling of the energy originally present in the different degrees of freedom so that the bias of the distribution with respect to the initial parallel energy is rapidly eliminated.

In a recent paper, Verheij *et al.*[11] studied distributions of emerging molecules for molecular beam scattering of CO on Pt(111) using pulse shape analysis. This enabled them to separate signals arising from processes with widely differing time delays. They found that for wide angle incidence, the angular distributions corresponding to fast processes displayed a strong main lobe and a diffuse component. They interpreted this in terms of direct scattering (main lobe) and re-emission from a physisorption region (diffuse component). They suggested that the surface potential displays a double minimum comprising separate chemisorption and physisorption regions into either of which incoming molecules may be trapped, thermalized and re-emitted. So far as we are aware, no other data have been presented that suggests an energy diagram of this form. The data of Verheij *et al.* were taken under incident conditions (65 meV incident energy, 585 K surface temperature) that preclude a direct comparison with our calculated distribution. However, the qualitative resemblance of the distribution in Fig. 5(b) with that given in Fig. 6 of Verheij *et al.* suggests that the observed fast diffuse component is due to molecules that emerge after making several round trips in the potential well, while the strong forward lobe devolves mainly from particles that traverse the well region only once. This interpretation is consistent with the observation that the diffuse fraction emerges with lower translational energy. In view of the high surface temperature ($kT_s \simeq 50$ meV), this fraction is effectively thermalized at the surface temperature for the low incident energy used in the experiments. However, complete thermalization would not be expected at incident CO energies of order 1 eV.

F. Comparison with other calculations

The calculations described above are limited in several respects and are intended merely to illustrate behavior rather than to allow a detailed comparison with experiment. More detailed calculations that are important in the present context[26,28] use the stochastic trajectory approach developed by Adelman and Doll.[29] Billing[26] considered explicitly the inelastic scattering of CO from Pt(111) and performed calculations for an incident angle of 45 deg, incident energies of 0.146, 5.0, 6.0 and 8.0 eV and surface temperatures in the range 20–1000 K. The calculated sticking coefficient at low incident energy and elevated surface temperature was found to be in the range 0.72–0.80. This suggests that the discrepancy between our calculations and the experiment at low energy in Fig. 4 can be attributed to surface temperature effects. At an incident energy of 5 eV, Billing found a sticking coefficient of about 0.3. Under similar incidence conditions, our model calculation gives upper and lower limits of 0.18 and 0.0 (i.e., sticking occurred only via the scudding channel). The difference between the two calculations may be due to translational–vibrational energy transfer, i.e., the molecule ceases to behave like a rigid rotor as the energy approaches the dissociation threshold. The interaction employed by Billing, though similar to that used in the present work at low energy, allowed for the possibility of CO dissociation. His finding that dissociation requires incident energies of order 8 eV is consistent with the complete absence of CO dissociation in our experiments at $E_i \leqslant 3.5$ eV.

Mulhausen *et al.*[28] discussed NO scattering from Ag(111) and Pt(111). They calculated angular distributions for NO/Ag(111), sticking probabilities as a function

of incident translational energy and the rotational distributions of scattered molecules. They stressed the importance of translational–rotational energy conversion on initial impact and showed that at low incident translational energy that translational–vibrational energy conversion is of minor importance. This is because of the relatively stiff vibrations and the tendency of the molecule to roll on hitting the surface, which weakens the force acting along the bond direction. The sticking coefficient for NO/Ag(111) was predicted to fall off with incident energy in a similar fashion to our finding for CO/Pt(111), but on a much smaller energy scale. The main reason for this difference is the smaller binding energy assumed for the NO/Ag(111) potential, and to differences in the form of the rotational corrugation. Mulhausen *et al.* assumed an angular anisotropy which produced a deep well only for $\gamma \simeq 0°$. The heights of the rotational corrugations relative to the binding energy are similar to those used here, but the two corrugations behave differently as a function of bond orientation and correspond to very different values of the well depth *averaged over bond orientation*. As a result, the net coupling between molecule and surface in the calculations of Mulhausen *et al.*, as compared with our calculations for CO/Pt(111), is weaker than the relative values of the binding energies would suggest. Comparison of Fig. 5 of Mulhausen *et al.* and Fig. 4 of the present paper demonstrate that the energy scale on which the sticking coefficient falls off depends on the form of the angular anisotropy as well as the maximum well depth.

IV. SUMMARY AND CONCLUSIONS

In summary, the experiments and calculations reported here suggest the following generalizations for understanding the scattering and sticking of molecular chemisorbed species from surfaces.

(1) For systems with well-depths of order 1 eV, the corrugation of the potential will generally be large and play an important role. The observation of a strong lobe about the specular direction in wide-angle scattering is a sign of the relative inefficiency of conversion or dissipation of the incident parallel energy, not that the surface is behaving like a mirror. A substantial amount of energy scrambling is the rule rather the exception and, as a result, the sticking coefficient is not likely to display behavior close to the normal energy scaling suggested by idealized flat-surface models. As a result, sticking coefficients would be expected to depend primarily on incident total energy and only weakly on incident angle.

(2) Translational-rotational conversion is expected to enhance sticking at energies well above the critical energy, but to suppress the sticking coefficient at lower energies. The suppression occurs because the excitation of the rotation weakens the coupling to lattice vibrations and reduces the energy transfer.

(3) Rotational and lateral corrugations lead to angular distributions for directly scattered particles at wide incident angles that display not only main lobes about the specular direction but also a diffuse component. The former component is due chiefly to trajectories that traverse the well region only once, while the diffuse fraction is due mainly to trajectories that trap on the first round trip and traverse the well region more than once. This observation may be important in connection with the extraction from experimental data of the relative fractions of direct scattering vs trapping–desorption.

ACKNOWLEDGMENTS

The authors gratefully acknowledge support via NATO Collaborative Research Grant No. 0834 and from the KFA Julich.

[1] F. O. Goodman and H. Y. Wachman, *Dynamics of Gas-Surface Scattering* (Academic, New York, 1976).
[2] J. E. Hurst, L. Wharton, K. C. Janda, and D. J. Auerbach, J. Chem. Phys. **78**, 1559 (1983).
[3] J. E. Hurst, C. A. Becker, J. P. Cowin, K. C. Janda, L. Wharton, and D. J. Auerbach, Phys. Rev. Lett. **43**, 1175 (1979).
[4] A. C. Luntz, M. D. Williams, and D. S. Bethune, J. Chem. Phys. **89**, 4381 (1988).
[5] C. T. Rettner, D. S. Bethune, and D. J. Auerbach, J. Chem. Phys. **91**, 1942 (1989).
[6] S. Andersson, L. Wilzén, M. Persson, and J. Harris, Phys. Rev. B (in press).
[7] M. Persson and J. Harris, Surf. Sci. **187**, 67 (1987).
[8] See, for example, A. C. Luntz, A. W. Kleyn, and D. J. Auerbach, in *Many-Body Phenomena at Surfaces*, edited by D. Langreth and H. Suhl (Academic, New York, 1984), p. 403.
[9] C. T. Campbell, G. Ertl, H. Kuipers, and J. Segner, Surf. Sci. **107**, 207 (1981).
[10] B. Poelsema, L. K. Verheij, and G. Comsa, Surf. Sci. **152-3**, 496 (1985).
[11] L. K. Verheij, J. Lux, A. B. Anton, B. Poelsema, and G. Comsa, Surf. Sci. **182**, 390 (1987).
[12] A. C. Luntz and D. S. Bethune, J. Chem. Phys. **90**, 1274 (1989).
[13] D. A. King and M. G. Wells, Proc. R. Soc. London Ser. A **339**, 245 (1974).
[14] F. P. Netzer and R. A. Willie, J. Catalysis **51**, 18 (1978).
[15] A. C. Luntz (unpublished).
[16] W. H. Weinberg and R. P. Merrill, JVST **8**, 718 (1972).
[17] M. P. D'Evelyn, H. P. Steinrück, and R. J. Madix, Surf. Sci. **180**, 47 (1987).
[18] S. L. Tang, J. D. Beckerle, M. B. Lee, and S. T. Ceyer, J. Chem. Phys. **84**, 6488 (1986).
[19] C. T. Rettner, H. Stein, and E. K. Schweizer, J. Chem. Phys. **89**, 3337 (1988).
[20] M. B. Lee, J. D. Beckerle, S. L. Tang, and S. T. Ceyer, J. Chem. Phys. **87**, 723 (1987).
[21] H. P. Steinrück, M. P. D'Evelyn, and R. J. Madix, Surf. Sci. **172**, L561 (1986).
[22] B. E. Hayden and D. C. Godfrey, J. Elect. Spectrosc. **45**, 351 (1987).
[23] Landolt-Börnstein, *Crystal and Solid State Physics*, Group III, Vol. 13 (Springer, Berlin, 1981).
[24] B. Persson and J. Mueller, Surf. Sci. **171**, 219 (1986).
[25] J. C. Tully, J. Chem. Phys. **73**, 6383 (1980).
[26] G. D. Billing, Chem. Phys. **86**, 349 (1984).
[27] J. Kimman, C. T. Rettner, D. J. Auerbach, J. A. Barker, and J. C. Tully, Phys. Rev. Lett. **57**, 2053 (1986).
[28] C. W. Mulhausen, L. R. Williams, and J. C. Tully, J. Chem. Phys. **83**, 2594 (1985).
[29] S. A. Adelman and J. D. Doll, J. Chem. Phys. **64**, 2375 (1976).